Conjugation Site Heterogeneity Causes Variable Electrostatic Properties in Fc Conjugates

Nicholas J. Boylan,[†] Wen Zhou,[†,§] Robert J. Proos,[†] Thomas J. Tolbert,[‡] Janet L. Wolfe,[†] and Jennifer S. Laurence*,[‡]

[†]Wolfe Laboratories, Inc., 134 Coolidge Avenue, Watertown, Massachusetts 02472, United States
[‡]Department of Pharmaceutical Chemistry, University of Kansas, Lawrence, Kansas 66047, United States

Ⓢ Supporting Information

ABSTRACT: Immunoconjugates, including antibody–drug conjugates and Fc-conjugates, represent a rapidly growing class of therapeutics undergoing clinical development. Despite their growing popularity, the high intrinsic heterogeneity of immunoconjugates often complicates the development process and limits their widespread application. In particular, immunoconjugate charge variants exhibit markedly different colloidal stabilities, solubilities, pharmacokinetics, and tissue distributions. Charge variants arise spontaneously due to degradation and, depending on the type of drug, linker, and conjugation site, through drug conjugation. Electrostatic changes in naked antibodies often result in poor performance characteristics, and therefore, charge alterations due to degradation are critical to control. Charge properties are expected to be equally important to producing well-behaved ADCs. Charge-based methods of analysis, such as isoelectric focusing and ion exchange chromatography, are capable of probing the underlying complexities within immunoconjugate drug products. Despite the utility of these methods, there are only a few published reports of charge-based assays applied to immunoconjugates. In the present study, we sought to identify the effects of chemical conjugation on the electrostatic properties of Fc-conjugates. In order to minimize the effects of post-translational modifications (e.g., deamidation), a single Fc charge variant was isolated prior to conjugation of a fluorescent probe, Alexa Fluor 350, to the side chains of lysine residues. The resulting Fc-conjugates were assessed by a variety of analytical techniques, including isoelectric focusing and ion exchange chromatography, to determine their charge properties.
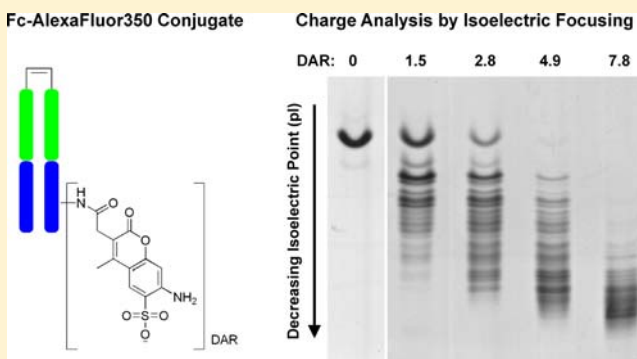
■ INTRODUCTION

Immunoconjugates, including antibody–drug conjugates (ADCs) and Fc-conjugates, represent a growing segment of the therapeutic candidates undergoing development.[1] ADCs combine the targeting specificity of monoclonal antibodies (mAbs) with the highly potent cytotoxic properties of small molecules for the treatment of cancer. A linker is used to covalently attach the cytotoxin to the mAb. Despite recent advances in engineering, design, and selection of ADCs,[1] intrinsic heterogeneity remains a major challenge, which can have a profound effect on the pharmacokinetics and tissue distribution of ADCs[2] as well as the physicochemical stability of the formulation.[3]

Biotherapeutics are inherently complex systems. During manufacturing, heterogeneities can be introduced due to enzymatic processing or spontaneous degradation.[4,5] Monoclonal antibodies are subject to post-translational modification, such as variable glycosylation, and routes of degradation, including deamidation, isomerization, oxidation, fragmentation, pyroglutamate formation, and aggregation.[4,6] These chemical and physical alterations often change the surface charge of mAbs.[4,5] Chemical conjugation, particularly when linking to

lysine, modifies the electrostatic properties of the mAb surface and introduces further complexities. Monoclonal antibodies often have 40–60 lysine residues, and chemical conjugation results in a heterogeneous mixture consisting of unconjugated mAbs and mAbs conjugated with a variable number of cytotoxins in random combinations at different sites on the antibody. Furthermore, chemical conjugation can potentially alter the hydrophobicity, charge, polarity, pharmacokinetics,[7] and thermostability of mAbs.[3,8] The inherent heterogeneity of ADCs remains a prominent challenge in characterizing their *in vivo* properties during development.[2]

To control heterogeneity, robust and reproducible manufacturing processes and appropriate analytical methods are required. Analytical characterization plays an important role in ensuring product integrity and manufacturing consistency,[4] which are essential for demonstrating safety and efficacy to the FDA and other regulatory authorities. However, the heterogeneity of ADCs makes analytical characterization particularly

challenging.[9] Selection of appropriate analytical techniques depends on the properties of the linker, the drug, and the choice of attachment site.[9] Analytical methods commonly used to assess the physicochemical properties of ADCs include mass spectrometry, chromatography, and electrophoresis. Here, we invoke a combination of these techniques to characterize the charge-based heterogeneity of a model immunoconjugate system. The system consists of IgG1 Fc conjugated with a fluorescent molecule, Alexa Fluor 350, via reaction with the solvent-accessible lysine residues.

EXPERIMENTAL PROCEDURES

Materials. Chemicals were obtained from Sigma-Aldrich unless otherwise noted. Deionized water (18 MΩ·cm) obtained from a Barnstead NANOpure Infinity water purification system was used to prepare all solutions.

Methods. *Expression and Purification of IgG1 Fc.* IgG1 Fc was expressed in a modified strain of SMD1168 *Pichia pastoris* and purified by protein G affinity chromatography as previously described.[10,11] Fc was buffer-exchanged into mobile phase A (10 mM Tris HCl, pH 9.0) using 10K MWCO Amicrometer Ultra-15 Centrifugal Filter Units (Millipore, Bedford, MA) and further purified via strong anion-exchange (SAX) chromatography. Approximately 0.5 mg of protein was loaded onto a Dionex ProPac SAX-10, 4 × 250 mm column (Sunnyvale, CA). Separation was achieved on a Shimadzu Prominence LC system (Tokyo, Japan) operated at 1 mL/min with a gradient of 99% A (10 mM Tris HCl, pH 9.0), 1% B (10 mM Tris HCl and 1 M NaCl, pH 9.0) to 90% A and 10% B over 25 min, followed by 1% A and 99% B over 1 min, which was then maintained for 5 min to wash the column. The column effluent was monitored at 280 nm. Fractions from 19 to 21 min were pooled (Figure S1, Supporting Information), concentrated, and buffer-exchanged into phosphate buffer (50 mM sodium phosphate and 50 mM NaCl, pH 7.3). The Fc concentration was determined by UV absorbance at 280 nm (molar extinction coefficient for Fc heavy chain = 35,785 M^{-1} cm^{-1}). Theoretical molar extinction coefficient and isoelectric point (pI) for IgG1 Fc were determined using the ProtParam tool within ExPaSy Proteomics Server of the Swiss Institute of Bioinformatics (http://www.expasy.ch/tools/protparam.html).[12]

Synthesis of Fc-Conjugates. Fc-conjugates were prepared at various dye-to-antibody ratios (DAR) by reacting Alexa Fluor 350 (AF350) carboxylic acid, succinimidyl ester (Molecular Probes, Eugene, OR) with the ε-amines of lysine residues following the manufacturer's instructions. Briefly, SAX-purified Fc was diluted to 2 mg/mL using appropriate volumes of reaction buffer A (100 mM sodium bicarbonate, 50 mM sodium phosphate, and 50 mM NaCl) and reaction buffer B (1,000 mM sodium bicarbonate, 50 mM sodium phosphate, and 50 mM NaCl) to achieve a final buffer composition of 100 mM sodium bicarbonate, 50 mM sodium phosphate, and 50 mM NaCl, pH 8.0. Subsequently, AF350 was dissolved in water (10 mg/mL) and immediately mixed with SAX-purified Fc at molar ratios of 0:1, 2.5:1, 5:1, 7.5:1, and 15:1 (dye-to-Fc ratio). The reaction proceeded for 1 h at ambient temperature under constant gentle stirring. Excess dye was subsequently removed by dialysis against phosphate buffer (50 mM sodium phosphate and 50 mM NaCl at pH 7.3) at 4 °C for 72 h using 10K MWCO Slide-A-Lyzer dialysis cassettes (Pierce, Rockford, IL). The resulting dye-to-antibody ratio (DAR) was determined by direct measurement of the protein absorbance at 280 nm and

dye absorbance at 346 nm and calculated using the following equation:

$$\text{DAR} = \frac{\varepsilon_{\text{Fc}}^{346} - R\varepsilon_{\text{Fc}}^{280}}{R\varepsilon_{\text{AF350}}^{280} - \varepsilon_{\text{AF350}}^{346}} \qquad (1)$$

where $\varepsilon_{\text{Fc}}^{280}$ = extinction coefficient of Fc at 280 nm (71,570 M^{-1} cm^{-1}), $\varepsilon_{\text{AF350}}^{280}$ = extinction coefficient of AF350 at 280 nm (3,610 M^{-1} cm^{-1}), $\varepsilon_{\text{Fc}}^{346}$ = extinction coefficient of Fc at 346 nm (determined to be negligible by relative UV absorbance measurement and therefore assumed to be zero), $\varepsilon_{\text{AF350}}^{346}$ = extinction coefficient of AF350 at 346 nm (19,000 M^{-1} cm^{-1}), and $R = A_{346}/A_{280}$ = the 346 to 280 nm absorbance ratio.[13] Subsequently, Fc-conjugates were diluted to 1 mg/mL in phosphate buffer (50 mM sodium phosphate, 50 mM NaCl at pH 7.3) and stored at 4 °C.

Characterization of Fc and Fc-Conjugates. Gel Electrophoresis. SDS−PAGE analysis was performed in NuPAGE 12% Bis-Tris precast gels with MOPS running buffer (Invitrogen, Carlsbad, CA). Analysis of IgG1 Fc and Fc-conjugates using reducing SDS−PAGE analysis resulted in two distinct bands. The higher intensity band corresponds to glycosylated protein (92%) and the less intense band to aglycosylated (8%) protein (Figure S2, Supporting Information).

Isoelectric focusing (IEF) was performed with Novex pH 3−10 precast IEF gels (Invitrogen). The gels were stained with Novex Colloidal blue staining kit according to the manufacturer's instructions. The stained gels were imaged using a GS-800 calibrated densitometer and analyzed with Quantity One Software (Bio-Rad Laboratories, Hercules, CA).

Size Exclusion (SE)-UPLC. Approximately 1 μg of protein was loaded onto an ACQUITY BEH125 SEC column (4.6 × 150 mm, 1.7 μm; Waters Corporation) equilibrated at 30 °C. All ultraperformance liquid chromatography (UPLC) separations were performed on a Waters ACQUITY H-Class BIO system (Milford, MA) equipped with tunable ultraviolet (TUV) and fluorescence detectors. Isocratic separation was performed (flow rate = 0.3 mL/min) with a mobile phase consisting of phosphate buffer (50 mM sodium phosphate and 50 mM NaCl, pH 7.3). The column effluent was monitored by UV detection at 280 and 346 nm and fluorescence detection at 346 nm (ex.) and 442 nm (em.).

Strong Anion Exchange (SAX)-UPLC. Approximately 10 μg of protein was loaded onto a Bio SAX-NP3 column (4.6 × 50 mm, 3 μm; Agilent Technologies) equilibrated at 30 °C. Gradient separation was achieved (flow rate = 0.5 mL/min) with an initial hold at 99% A (10 mM Tris HCl, pH 9.0), 1% B (10 mM Tris HCl and 1 M NaCl, pH 9.0) for 3 min, followed by 38% A, 62% B over 67 min, 1% A, 99% B over 5 min, then 99% A, and 1% B over 1 min, which was then maintained for 4 min to re-equilibrate the column. The column effluent was monitored by UV detection at 280 and 346 nm and fluorescence detection at 346 nm (ex.) and 442 nm (em.).

Liquid Chromatography−Electrospray Mass Spectrometry (LC-ESI-MS). The ESI-MS system was an Applied Biosystems 4000 QTrap equipped with an electrospray ionization source (Applied Biosystems, Foster city, CA). The instrument was operated in positive ion mode and scanned from 1190 to 1470 m/z. The mass accuracy and resolution of the method were <100 ppm and 1200, respectively. The tandem mass spectrometer (MS/MS) system was coupled to two LC-20AD pumps with an in-line CBM-20A controller, a DGU-

20A5 solvent degasser (Shimadzu, Kyoto, Japan), and a LEAP CTC HTS PAL autosampler (CTC Analytics, Carrboro, NC).

To simplify the mass spectrum, samples were deglycosylated and reduced prior to analysis. Deglycosylation was performed by incubating 50 μg of sample with 1.25 U of N-glycosidase F (EMD Millipore, Billerica, MA) at room temperature overnight. The samples were subsequently reduced with 20 mM dithiothreitol (DTT) at 37 °C for 1 h. Approximately 10 μg of deglycosylated, reduced sample was loaded onto an Agilent Zorbax SB-C8 HPLC column (4.6 × 150 mm, 3.5 μm) equilibrated at 40 °C. Gradient separation was achieved (flow rate = 1 mL/min) with an initial hold at 95% A (0.1% formic acid in water), 5% B (0.1% formic acid in acetonitrile) for 1 min, followed by 5% A, 95% B over 3 min, held at 5% A, 95% B for 2 min, then back to 95% A, 5% B over 3 min, which was then maintained for 3 min to re-equilibrate the column. Because of protein carryover, the column was washed between runs, and at least one blank injection was performed between any two consecutive protein injections.

Peak assignments were performed by comparison of theoretical and observed mass-to-charge ratios in the range of 1190 to 1470 m/z (Tables S1–S4, Supporting Information). The protein sequence and glycosylation states were identified under reducing conditions, with and without PNGase F treatment, via LC-ESI-MS (data not shown). Multiple peaks were observed that correspond to aglycosylated and high-mannose Fc glycoforms, in good agreement with previous reports.[10] Characterization of deglycosylated and reduced Fc-conjugates by LC-ESI-MS resulted in the identification of peaks corresponding to Fc heavy chain conjugated with 0–8 AF350 molecules (threshold set at 3.0 × 10^4 cps) (Figure S3A–D, Supporting Information). With the exception of Fc heavy chain peaks in the 20+ charge state, the mass spectra were complicated by peak overlap between neighboring charge states (e.g., overlap of peaks corresponding to Fc heavy chain conjugates with 4 and 0 AF350 molecules in the 22+ and 21+ charge states, respectively). Thus, only peaks corresponding to the Fc heavy chain in the 20+ charge state were used for quantitative analysis.

Statistical Analysis. All statistical analyses were performed using SPSS statistical software, version 18.0 (SPSS Inc., Chicago, IL). The Pearson product–moment correlation coefficient (r) was used to determine the linear dependence between variables. Differences were considered to be statistically significant at a level of $P < 0.05$.

◼ RESULTS

Purification and Characterization of IgG1 Fc. To evaluate the effects of chemical conjugation on the charge properties of Fc-conjugates, the charge heterogeneity of IgG1 Fc was assessed prior to chemical conjugation with AF350. Analysis of protein G affinity-purified Fc using nonreducing, nondenaturing isoelectric focusing (IEF) revealed the presence of five bands, including two acidic and two basic Fc isoforms (Figure 1). The most prominent band has an isoelectric point (pI) of approximately 7.7 ± 0.07, which is 0.6 units greater than the theoretical value calculated from the protein sequence (Table S5, Supporting Information). This level of heterogeneity would complicate the Fc-conjugate charge profile and mask effects due to chemical conjugation. To reduce the number of charge variants, IgG1 Fc was further purified using SAX-HPLC and determined by IEF to consist of a single charge species with a pI of approximately 7.7 (Figure 1). LC-MS confirmed that the
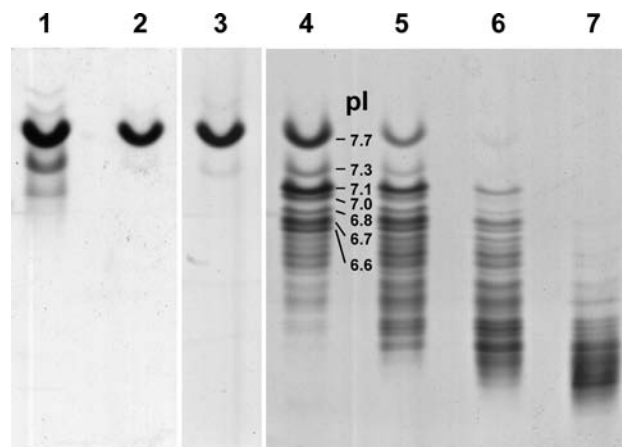
Figure 1. IEF analysis of IgG1 Fc and Fc-conjugates. Lanes: 1, protein G affinity-purified IgG1 Fc; 2, SAX purified IgG1 Fc and Fc-conjugates; 3, DAR 0; 4, DAR 1.5; 5, DAR 2.8; 6, DAR 4.9; and 7, DAR 7.8. The isoelectric point (pI) for the labeled bands were identified using the SERVA IEF marker 3–10 from Invitrogen.

major band corresponds to native Fc. The yield of SAX-purified Fc was ∼68%. This is in good agreement with IEF band analysis of protein G affinity-purified Fc, which contained ∼68% native Fc as determined by densitometry.

Analysis of Average Dye-to-Antibody Ratio (DAR). An important factor influencing the efficacy and stability of immunoconjugates is the average number of drug molecules covalently attached to the protein carrier. The average dye-to-antibody ratio (DAR) was determined using UV/Vis spectroscopy. Figure 2 shows the normalized absorption spectra of the
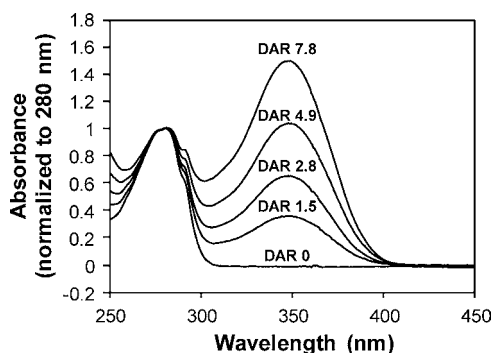
Figure 2. UV spectra of Fc-conjugates prepared at various DARs, normalized to absorbance at 280 nm. The overlay shows a proportional increase in 346 nm absorbance as the amount of conjugated AF350 increases.

Fc-conjugates at various labeling densities. With increasing DAR, the absorption band of IgG1 Fc at 280 nm decreases relative to the absorption band of the AF350 at 346 nm. Using the extinction coefficients for Fc and AF350 at their absorption maxima, the average DARs are 0, 1.5, 2.8, 4.9, and 7.8 (Table 1). This range encompasses the typical DAR values encountered in ADCs; in general, a DAR of 2–4 results in the best therapeutic window.[13–15]

The average DAR was also determined by integrating the absorbance during SE-UPLC chromatographic separation (Figure 3). Using eq 1 and by taking the ratio of the area under the curves (346 to 280 nm), the average DARs were in good agreement with results obtained using the cuvette-based

Table 1. Characterization of Fc-Conjugates

reaction stoichiometry[a]	average DAR[b]	range of DAR species[c]	yield, %[d]	purity, %[e]
2.5	1.5 ± 0.02	0−8	83	99.9
5.0	2.8 ± 0.04	0−10	89	98.6
7.5	4.9 ± 0.05	0−12	86	99.5
15	7.8 ± 0.01	2−16	86	97.4

[a]Stoichiometric ratio of Alexa Fluor 350 to Fc protein during the conjugation reaction. [b]Average dye-to-antibody ratio (DAR) as determined by UV/Vis spectroscopy. Data represents the average ± SD (*n* = 2). [c]Range of dye-to-antibody ratios observed for Fc-conjugates as determined by LC-ESI-MS analysis of deglycosylated and reduced protein samples. [d]Yield of Fc-conjugates post-dialysis against phosphate buffer at 4 °C for 72 h using 10K MWCO Slide-A-Lyzer dialysis cassettes. [e]Percentage of conjugate dye (as compared to free dye) as determined by SE-UPLC analysis with fluorescence detection.
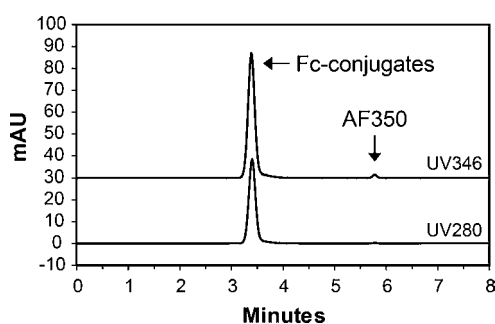
Figure 3. Analysis of native Fc-conjugate DAR 7.8 via SE-UPLC with UV absorbance detection at 280 and 346 nm. Labeled peaks correspond to unconjugated AF350 and Fc-conjugates.

method (Table 2). Additionally, SE-UPLC also allows for the detection of protein aggregates and low molecular weight

Table 2. Comparison of Average Dye-to-Antibody Ratios Measured by Various Methods

DAR via UV−Vis[a]	DAR via SE-UPLC (AUC)[a]	DAR via LC-MS	FWHM[b]
1.5 ± 0.02	1.4 ± 0.01	1.6	3.1
2.8 ± 0.04	2.8 ± 0.02	3.0	4.3
4.9 ± 0.05	4.8 ± 0.02	5.1	5.0
7.8 ± 0.01	7.7 ± 0.02	8.3	5.3

[a]Data represents the average ± SD (*n* = 2). [b]Full width at half-maximum (FWHM) obtained from the DAR distributions shown in Figure 4.

impurities, which can result in undesirable immunogenicity and/or decreased efficacy.[16] Analysis of peak shape and elution time indicated that no soluble Fc aggregates were present and that samples contained less than 5% unconjugated dye. Although these techniques enable accurate measurement of the average properties of immunoconjugates, both approaches lack the ability to probe heterogeneity among the conjugates.

To begin to characterize the individual DAR components of the Fc-conjugate pool, LC-ESI-MS was used as an orthogonal method. First, the average DAR values were examined and compared to the values derived from the absorbance methods. Mass peaks corresponding to the Fc heavy chain conjugated with 0−*n* AF350 molecules were detected for each sample (Figure S3A−D and Tables S1−S4, Supporting Information).

To account for the potential change in ionization properties of the conjugate relative to the naked protein and between different conjugate species, the quantitative analysis of ADCs by ESI-MS should include all of the charge states for each conjugate species.[17] However, due to the inability to resolve overlapping peaks between neighboring charge states (e.g., overlap of peaks corresponding to Fc heavy chain conjugates with 4 and 0 AF350 molecules in the 22+ and 21+ charge states, respectively), it was not possible to definitively quantify the individual conjugate species in all of the charge states. Therefore, the average DAR was estimated by integration of the peaks corresponding to the Fc heavy chain in 20+ charge state. Assuming equivalent recovery and ionization of all species, the average DAR was calculated according to the following equation:

$$DAR = 2 \times \sum (n \times An) / \sum (An) \tag{2}$$

where *n* equals the number of AF350 molecules per Fc chain, and *An* is the peak area corresponding to the species with *n* AF350 molecules per Fc chain.[17] The average DAR determined from MS data was within 8% of the UV-based approaches, with the exception of Fc-conjugate DAR 1.4, which was within 12% (Table 2). Similar results were obtained from MS data collected in the range of 1380−1660 *m/z* for the resolvable 17+ and 18+ charge states, but peak overlap prevented quantitation of all charge states (data not shown). Together, these results indicate that the current LC-ESI-MS analytical method, while not highly accurate, reasonably estimates the average DAR of Fc-conjugates.

Analysis of Individual DAR Species by Mass Spectroscopy. In addition to average DAR, characterizing the distribution of individual DAR species is important because different forms may have different behaviors, including stability, PK, and toxicity profiles.[13] Analysis of deglycosylated and reduced Fc-conjugates by LC-ESI-MS shows a wide distribution of the number of AF350 molecules conjugated to each Fc chain. The relative abundance of each species (*Xn*) was calculated according to the following equation:

$$Xn = (An) / \sum (An) \tag{3}$$

where *n* equals the number of AF350 molecules per Fc heavy chain, *Xn* is the fraction of heavy chains molecules conjugated with *n* number of AF350 molecules per chain, and *An* is the peak area corresponding to that species. Because a normal distribution of DAR species is expected to result from the chemistry, the DAR distribution of intact Fc-conjugates was predicted using probability theory, and the relative abundance of each individual DAR species was compared. As shown in Figure 4, the predicted DAR distributions for intact Fc-conjugates are plotted along with corresponding normal distributions. As expected, an increase in the average DAR resulted in an increase in the number of individual DAR species (*r* = 0.986), which is consistent with the normal probability distribution function. The dependence of heterogeneity on average DAR is also described by the full width at half-maximum (FWHM) for each DAR distribution, which increased with increasing average DAR (Table 2). Together, these data indicate the expected range and proportion of individual DAR species produced for each sample (Figure 4).

Charge Analysis by IEF and SAX-UPLC. Prior to SAX purification, charge-based analysis of IgG1 Fc resulted in the presence of native Fc along with two acidic and two basic
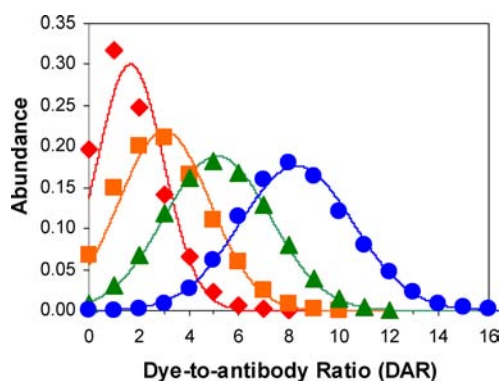
Figure 4. Distribution of DAR species. Symbols represent the relative abundance of each individual DAR species as determined by LC-ESI-MS analysis of reduced and deglycosylated Fc-conjugates. The diamonds (red), squares (orange), triangles (green), and circles (blue) represent Fc-conjugates with average DAR values of 1.5, 2.8, 4.9, and 7.8, respectively. Solid lines in the same color represent the theoretical normal distribution for the corresponding average DAR.

isoforms. The shift in pI for the two acidic bands observed at 7.4 and 7.1 corresponds to the theoretical shift in pI upon deamidation of one and two asparagine (Asn) residues, respectively. This is expected because the protein sequence contains two Asn-Gly motifs that are highly susceptible to deamidation.[18] The basic isoforms may be attributed to other post-translational modifications such as oxidation, isomerization, and formation of the succinimide intermediate during deamidation.[4] In general, this level of charge heterogeneity is typical of commercially prepared biotherapeutics.[5,19−21] Here, these degradation products were effectively removed by SAX, permitting an analysis of how conjugation affects charge behavior.

Chemical conjugation, particularly when linking to lysine residues, modifies the electrostatic properties of the Fc protein surface. Thus, the electrostatic properties of Fc-conjugates were assessed using IEF. Despite starting with homogeneous SAX-purified Fc, IEF analysis of the Fc-conjugate DAR 0 (mock reaction) had a small proportion (0.9%) of an additional acidic band. This band likely corresponds to deamidated Fc, which forms spontaneously during storage in near neutral conditions (Figure 1). In this study, conditions were controlled carefully to limit the extent of deamidation in the conjugate samples to below or near the limit of detection of the methods used to eliminate interference and focus on changes resulting from the attachment of AF350.

Chemical conjugation with AF350 resulted in a reduction in the pI of conjugated versus unconjugated species. Because of the decrease in pI upon conjugation, the amount of unconjugated versus conjugated protein is readily quantified by IEF analysis. The percentage of naked Fc in Fc-conjugates DAR 1.5 and DAR 2.8 was 21.6 and 5.3%, respectively, whereas, no naked Fc was detected in Fc-conjugates DAR 4.9 and DAR 7.8. In general, Fc-conjugates displayed a very complex pI profile. If the distribution of DAR species was the only factor determining the charge properties upon conjugation, then only 6 additional bands corresponding to DAR 1−6 (DAR 7 and 8 are below the IEF limit of detection) would be expected for Fc-conjugate DAR 1.5. However, approximately 14 additional bands were observed for Fc-conjugate DAR 1.5 by IEF (Figure 1), indicating that DAR distribution is not the sole factor influencing the charge properties.

Above pH 3.8, AF350 carries a net negative charge due to the presence of a sulfonate group. Therefore, conjugation of AF350 to the ε-amine of lysine is expected to reduce the net charge by two at neutral pH. The theoretical pIs for Fc-conjugates with 0−8 AF350 molecules were estimated by substituting aspartic acid for lysine within the protein sequence and inputting the sequence into the ProtParam tool (ExPaSy Server) (Table S5, Supporting Information). Because native Fc displays a pI that differs substantially from the theoretical value, addition of a correction factor of 0.6 was applied to account for the difference. The estimated pI for Fc-conjugated with the 1-AF350 molecule is 7.2, which corresponds to the most intense band present in Fc-conjugate DAR 1.5 at pI 7.1. Interestingly, the pI of the third most intense band for Fc-conjugate DAR 1.5 is 6.7, which approximately corresponds to the predicted pI of 6.9 for Fc-conjugated with 2-AF350 molecules. Analysis of the IEF lane profile for Fc-conjugate DAR 1.5 shows the presence of two additional bands (pI ∼7.3 and 7.0) that are adjacent to the major DAR 1 band and two additional bands (pI ∼6.8 and 6.6) that are adjacent to the major DAR 2 band (Figure 1). Although the band at pI ∼7.3 migrates with the deamidated Fc band observed in the mock reaction, the relative abundance of the individual deamidated species after the conjugate reaction is below the limit of detection, indicating that this band instead results from AF350 attachment. Assuming these neighboring bands represent charge variants with the same number of attached dye molecules, the total relative abundance of DAR 1 and DAR 2 is 33% and 25%, respectively, which is in good agreement with the DAR distribution determined by mass spectrometry. For DAR 1, the major band at pI 7.1 constitutes 68% of the DAR 1 species, while the less intense bands at pI 7.3 and 7.0 represent 15% and 17% of the total subpopulation, respectively. Similarly, 52% of DAR 2 has a pI of 6.7, and the bands at pI 6.8 and 6.6 represent 19% and 29% of the DAR 2 conjugates, respectively. IEF analysis of Fc-conjugate DAR 2.8 resulted in the identification of 19 bands corresponding to species conjugated with 1−8 AF350 molecules (DAR 9 and 10 are below the IEF limit of detection). As the average DAR increased to 4.9 and 7.8, there was a shift in the band intensities to more acidic charge variants (higher DAR species). In general, the theoretical pIs (with applied correction factor) agreed well with the observed values for bands corresponding to Fc-conjugate DAR 1 and 2. Above DAR 2, the observed pIs could not be identified using this approach. In addition, the relative quantities of Fc-conjugates DAR 1−2 were in good agreement with the DAR distribution predicted by mass spectrometry. However, due to substantial band overlap, the number of resolvable individual IEF bands decreased as the average DAR increased from 2.8 to 7.8. Positional isomers likely account for the high charge heterogeneity. Assuming all 38 lysine residues are available for conjugation, for example, using the binomial coefficient, there are more than 10^3 and 10^7 positional isomers for the attachment of 3 and 8 molecules, respectively, to Fc. The actual number of isoforms is greatly expanded because a range of DARs is present. Despite the high heterogeneity, the majority of Fc-conjugate species show similar charge properties. It is, however, evident in the average DAR 1.5 and 2.8 samples that a few distinct subpopulations emerge for an individual DAR, which indicates that not every conjugate behaves in the same manner. Fc-conjugates species with higher average DAR values exhibit a more complex spectrum of charge properties, and identification of the individual species is hindered by decreased resolution. As a result, we were unable

to assign DAR values to the more acidic bands corresponding to Fc-conjugates with DAR ≥ 3.

In addition to IEF analysis, SAX-UPLC was used as an orthogonal method to assess the electrostatic properties of Fc-conjugates. The elution of Fc and Fc-conjugated species were monitored by UV absorbance at 280 nm, whereas conjugate and unconjugated AF350 species were monitored by UV absorbance at 346 nm and fluorescence emission. Analysis of Fc-conjugate DAR 0 (mock reaction) resulted in a single peak that eluted at 13 min (Figure S4A, Supporting Information). Unlike IEF, no additional peak corresponding to deamidated Fc was observed because the UV signal intensity was below the limit of detection. As expected, chemical conjugation with AF350 increased the retention time of Fc-conjugated species due to increased interaction between the anionic AF350 molecules and the cationic column packing material (Figure 5).
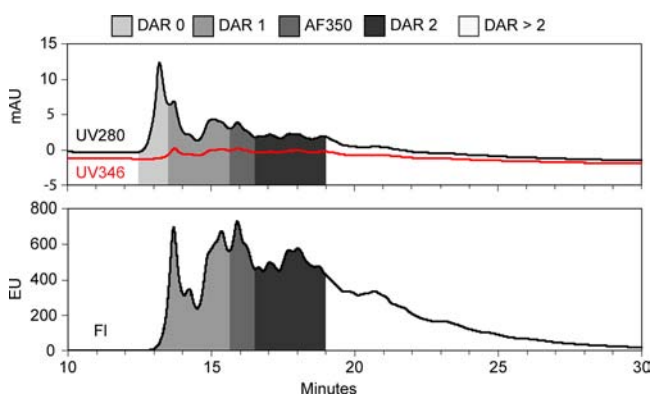
Figure 5. Analysis of Fc-conjugate DAR 1.5 via SAX-UPLC. Overlay of individual 280 and 346 nm absorbance traces (top) and fluorescence detected at 442 nm (bottom) are shown. Shaded areas represent unconjugated AF350 and Fc-conjugates with calculated dye-to-antibody ratio derived from measured absorbance at 346 nm (dye) and 280 nm (Fc).

In general, Fc-conjugates displayed very complex peak profiles by SAX-UPLC. Although, baseline resolution of each variant was not achievable, we were able to identify peaks based on the relative contributions from protein and AF350 signals. Thus, the amount of unconjugated versus conjugated protein was readily quantified by SAX-UPLC. The percentage of naked Fc in DAR 1.5 and DAR 2.8 samples was 22% and 3.6%, respectively, whereas, no naked Fc was detected in DAR 4.9 and DAR 7.8 samples. These values are in good agreement with the IEF analysis. The peak corresponding to unconjugated AF350 was identified at 16 min (Figures S4B, Supporting Information) and was determined to be less than 5% of the total UV 346 nm peak area for Fc-conjugates, in agreement with SE-UPLC analysis. Additionally, each peak was assigned a DAR value using eq 1 by taking the ratio of the baseline-corrected UV 346 nm and UV 280 nm channels. For Fc-conjugate DAR 1.5, peaks corresponding to Fc conjugated with 0 to 2 AF350 molecules were observed; those with larger DARs were below the limit of detection. For species with DAR < 3, multiple peaks are apparent. On the basis of the absorbance ratio, 3 peaks in the fluorescence trace were identified that correspond to DAR 1 (Figure 5). Because of significant overlap among Fc-conjugate species with DAR > 2, it was difficult to resolve individual species. This is not surprising because the site of conjugation and orientation of the conjugated AF350

molecule likely influence the resulting interaction between the conjugate and column matrix. Regardless, the increased sensitivity afforded by fluorescence detection identified the presence of low abundance species that eluted later and likely correspond to Fc-conjugates with DARs of 3−8, which were observed using MS. Similarly, SAX-UPLC analysis of Fc-conjugate DAR 2.8 resulted in peaks corresponding to Fc conjugated with 0 to 4 AF350 molecules before the UV signal intensities dropped below the limit of detection (Figure S4C, Supporting Information). As the average DAR increased to 4.9 and 7.8, there was a further shift in the elution time and increased peak overlap, likely due to an increase in the number of DAR species and charge variants (Figures S4D and S4E, Supporting Information). Comparison of the absorbance ratios provides confirmation that a range of charge behaviors emerge among individual DAR subpopulations.

■ DISCUSSION

The electrostatic properties of a protein, including pI and charge distribution, are critical parameters that influence protein behaviors such as thermal stability[22−24] and viscosity,[25,26] and as such, it is important to assess the charge properties of protein therapeutics, including immunoconjugates. In the present study, we sought to characterize the effects of attaching AF350 to IgG1 Fc on electrostatic properties of the resulting Fc-conjugates. Charge-based methods of analysis, such as IEF and SAX-UPLC, are capable of probing the underlying complexities within immunoconjugate drug products. Despite the utility of these methods, there are only a few published reports of charge-based assays applied to immunoconjugates.[9,27−29] This may be in part because of the high charge heterogeneity of conjugates because charge variants may arise spontaneously due to chemical degradation and as a result of modification. Here, isolation of the native, single-charge variant of Fc was performed to simplify analysis and examine the effects of chemical conjugation on the observed charge of Fc using IEF and SAX-UPLC. Using this approach, we demonstrated the existence of multiple charge variants within a single DAR.

The choice of chemistry used to link the protein carrier and payload is critical for the success of immunoconjugates.[30] Conjugation strategies often involve reaction to solvent accessible lysine residues.[30] A number of ADCs undergoing late-stage clinical trials utilize lysine-based linker chemistries and include Trastuzumab emtansine[3] and Inotuzumab ozogamicin.[31] Because of favorable reaction kinetics and stability of the resulting amide bond, chemical cross-linking reactions commonly use succinimidyl ester chemistry to react with the ε-amine of lysine residues.[30] Therefore, we used a succinimidyl ester of AF350 to react with the ε-amine of lysine residues. On the basis of the protein sequence, 38 lysines are theoretically available for conjugation. Because of the random nature of chemical conjugation with solvent accessible lysine residues,[17,32] it was anticipated that the resulting Fc-conjugates would consist of a complex mixture of species that differ in both the number of conjugated AF350 molecules and sites of covalent attachment, consistent with a normal distribution.

We anticipated that the number of dye molecules attached, rather than the site of attachment to Fc would dictate the overall charge of the conjugate and therefore would be predictable. The results of the SAX and IEF analyses, however, indicate that more than one charge state exists for individual Fc-conjugates having the same DAR. This is most easily

observed in the sample with the lowest average DAR (1.5). Comparison of the absorbance intensities of the protein and dye for a given SAX peak demonstrates that attachment of a single dye molecule results in more than one peak position. This reflects a difference in the overall charge behavior of individual conjugates and suggests that some site(s) of attachment may have an additional influence on electrostatic properties of the conjugate. This is also observed when two or more dye molecules are attached, but the analysis becomes more complex as crowding decreases resolution, and combinations of individual DARs may overlap. Similarly, IEF analysis of Fc-conjugates resulted in additional bands, indicating that DAR is not the only factor influencing the charge behavior. Thus, the local protein environment, which is known to influence the pK_a of resident amino acids, may perturb a network of charge-based interactions on Fc and/or influence the pK_a of conjugated AF350. The importance of context surrounding a charged moiety was highlighted in the classical work of Tanford et al.[33−35] Furthermore, chemical conjugation may indirectly affect the pI through alteration of the higher order protein structure. Therefore, the high charge heterogeneity is likely due to a combination of DAR distribution and site of conjugation.

Another important parameter for therapeutic immunoconjugates is the average number of drug molecules covalently attached to the protein carrier.[17] Multiple methods, including UV absorbance spectrophotometry and mass spectrometry, were used to measure the average DAR values. In general, these orthogonal methods resulted in comparable average DAR values. Although we did not expect MS quantification of DAR to be highly accurate due to peak overlap, which prevented analysis of all charge states, the distribution of individual DAR species was reasonably estimated. The range of individual DAR species increased with average DAR and is likely a direct result of the choice of reaction chemistry, which is relatively nonspecific due to the availability of ∼38 reaction sites per Fc protein. Approximately 70% of the DAR 1 species behaved as expected, but interestingly, 30% of protein with DAR 1 did not. Two additional charge behaviors were observed for DAR 1. This trend was detected for DAR 2 as well. Although species with DAR greater than 2 were not quantified due to insufficient resolution, the combined SAX, IEF, and MS analyses indicate that the trend continues because the charge behavior is more complex than predicted by DAR alone.

Although further studies are required to characterize the positions at which conjugation alters the charge behavior of Fc, it is reasonable to hypothesize that partially exposed lysine residues involved in electrostatic interactions are most likely responsible because neither protein loss nor aggregates were observed. Conjugation with these lysine residues could alter the conformation of the protein and/or expose previously paired, negatively charged residues, which would shift the pI to a slightly more acidic value than that when an unpaired lysine is modified. Because the measured pI is substantially more basic than predicted from the sequence, even a modest conformational change could perturb the synergy of the electrostatic network, likely resulting in a shift toward a more acidic pI. Alternatively, a specific salt bridge could be broken. As noted by Liu et al., the crystal structure of human IgG1 Fc[36] reveals direct hydrogen bonding between K29 and E161 in the CH2-CH3 hinge region.[37] Modification of this surface accessible lysine would leave the carboxylate without a binding partner. Similarly, Gunasekaran et al. identified a pair of peripherally

located charged residues (K409-D399) at the interface of the CH3 domains.[38] In this case, K409 is not completely buried but is less surface accessible than K29. Breaking the electrostatic association at this site would alter the domain−domain interface and increase exposure of the anionic partner. These two types of interactions likely affect the pI to different extents because of differences in packing and could potentially explain the observation of two subpopulations of charged states for DAR 1.

A lack of understanding and control of conjugation site can lead to charge heterogeneity, which affects pharmaceutical and biopharmaceutical properties as well as efficacy. The effects of charge heterogeneity on the thermal stability, solubility, and viscosity of mAbs are well documented[22−26] and have established the need for the detection of and implementation of measures to control charge properties that affect critical quality attributes. Such studies have not yet been reported for ADCs. To better inform discovery and ensure product integrity, further studies are required to understand the factors responsible for the impact of charge heterogeneity of ADCs. Follow up studies, including purification of individual Fc-conjugate charge variants and subsequent peptide mapping analysis, are expected to reveal the specific conjugation sites responsible for the observed charge heterogeneity.

■ CONCLUSIONS

It is known that lysine-based conjugation results in a highly heterogeneous mixture of molecules, which vary in the distribution of DAR and site of attachment. Here, we provide evidence that the position at which a small molecule is attached to the Fc protein affects the overall charge of the conjugate, independent of DAR. Subpopulations were observed for species having the same number of conjugated molecules that differ in their overall charge. This led to greater heterogeneity in the electrostatic properties of the conjugates than would be expected based solely on the number of lysine residues modified. As has been shown with mAbs, electrostatic properties affect the stability, solubility, and viscosity of proteins. As such, the ability to characterize charge properties of ADCs is important for evaluating their performance characteristics and to reliably generate stable, well-behaved protein−drug conjugates.

■ ASSOCIATED CONTENT

Ⓢ Supporting Information

Additional information as noted in the text. This material is available free of charge via the Internet at http://pubs.acs.org.

■ AUTHOR INFORMATION

Corresponding Author

*Department of Pharmaceutical Chemistry, The University of Kansas, Multidisciplinary Research Building, 2030 Becker Dr., Lawrence, KS 66047. Phone: 785-864-3405. Fax: 785-864-5736. E-mail: laurencj@ku.edu.

Present Address

§W.Z.: BioScience, Baxter Healthcare Corporation, 1700 Rancho Conejo Boulevard, Thousand Oaks, CA 91320.

Notes

The authors declare no competing financial interest.

■ ABBREVIATIONS

ADC, antibody−drug conjugate; AF350, Alexa Fluor 350; DAR, dye-to-antibody ratio; HPLC, high performance liquid chromatography; IEF, isoelectric focusing; IgG1 Fc, fragment crystallizable region of immunoglobulin G subtype 1; LC-ESI-MS, liquid chromatography−electrospray mass spectrometry; mAb, monoclonal antibody; pI, isoelectric point; SAX, strong anion-exchange; SDS−PAGE, sodium dodecyl sulfate−polyacrylamide gel electrophoresis; SE, size-exclusion; UPLC, ultraperformance liquid chromatography; UV, ultraviolet

■ REFERENCES

(1) Sapra, P., Hooper, A. T., O'Donnell, C. J., and Gerber, H.-P. (2011) Investigational antibody drug conjugates for solid tumors. *Expert Opin. Invest. Drugs 20*, 1131−1149.

(2) Boswell, C. A., Mundo, E. E., Zhang, C., Bumbaca, D., Valle, N. R., Kozak, K. R., Fourie, A., Chuh, J., Koppada, N., Saad, O., Gill, H., Shen, B.-Q., Rubinfeld, B., Tibbitts, J., Kaur, S., Theil, F.-P., Fielder, P. J., Khawli, L. A., and Lin, K. (2011) Impact of drug conjugation on pharmacokinetics and tissue distribution of anti-STEAP1 antibody−drug conjugates in rats. *Bioconjugate Chem. 22*, 1994−2004.

(3) Wakankar, A. A., Feeney, M. B., Rivera, J., Chen, Y., Kim, M., Sharma, V. K., and Wang, Y. J. (2010) Physicochemical stability of the antibody-drug conjugate Trastuzumab-DM1: changes due to modification and conjugation processes. *Bioconjugate Chem. 21*, 1588−1595.

(4) Vlasak, J., and Ionescu, R. (2008) Heterogeneity of monoclonal antibodies revealed by charge-sensitive methods. *Curr. Pharm. Biotechnol. 9*, 468−481.

(5) Khawli, L. A., Goswami, S., Hutchinson, R., Kwong, Z. W., Yang, J., Wang, X., Yao, Z., Sreedhara, A., Cano, T., Tesar, D. B., Nijem, I., Allison, D. E., Wong, P. Y., Kao, Y.-H., Quan, C., Joshi, A., Harris, R. J., and Motchnik, P. (2010) Charge variants in IgG1: Isolation, characterization, in vitro binding properties and pharmacokinetics in rats. *MAbs 2*, 613−624.

(6) Liu, H., Gaza-Bulseco, G., Faldu, D., Chumsae, C., and Sun, J. (2008) Heterogeneity of monoclonal antibodies. *J. Pharm. Sci. 97*, 2426−2447.

(7) Boswell, C. A., Tesar, D. B., Mukhyala, K., Theil, F.-P., Fielder, P. J., and Khawli, L. A. (2010) Effects of charge on antibody tissue distribution and pharmacokinetics. *Bioconjugate Chem. 21*, 2153−2163.

(8) Acchione, M., Kwon, H., Jochheim, C. M., and Atkins, W. M. (2012) Impact of linker and conjugation chemistry on antigen binding, Fc receptor binding and thermal stability of model antibody-drug conjugates. *MAbs 4*, 362−372.

(9) Wakankar, A., Chen, Y., Gokarn, Y., and Jacobson, F. S. (2011) Analytical methods for physicochemical characterization of antibody drug conjugates. *MAbs 3*, 161−172.

(10) Xiao, J., Chen, R., Pawlicki, M. A., and Tolbert, T. J. (2009) Targeting a homogeneously glycosylated antibody Fc to bind cancer cells using a synthetic receptor ligand. *J. Am. Chem. Soc. 131*, 13616−13618.

(11) Nett, J. H., and Gerngross, T. U. (2003) Cloning and disruption of the PpURA5 gene and construction of a set of integration vectors for the stable genetic modification of Pichia pastoris. *Yeast 20*, 1279−1290.

(12) Gasteiger, E., Hoogland, C., Gattiker, A., Duvaud, S. E., Wilkins, M. R., Appel, R. D., and Bairoch, A. (2005) Protein Identification and Analysis Tools on the ExPASy Server, in *The Proteomics Protocols Handbook* (Walker, J. M., Ed.) pp 571−607, Humana Press, New York.

(13) Hamblett, K. J., Senter, P. D., Chace, D. F., Sun, M. M., Lenox, J., Cerveny, C. G., Kissler, K. M., Bernhardt, S. X., Kopcha, A. K., Zabinski, R. F., Meyer, D. L., and Francisco, J. A. (2004) Effects of drug loading on the antitumor activity of a monoclonal antibody drug conjugate. *Clin. Cancer Res. 10*, 7063−7070.

(14) Ducry, L., and Stump, B. (2009) Antibody−drug conjugates: linking cytotoxic payloads to monoclonal antibodies. *Bioconjugate Chem. 21*, 5−13.

(15) McDonagh, C. F., Turcott, E., Westendorf, L., Webster, J. B., Alley, S. C., Kim, K., Andreyka, J., Stone, I., Hamblett, K. J., Francisco, J. A., and Carter, P. (2006) Engineered antibody−drug conjugates with defined sites and stoichiometries of drug attachment. *Protein Eng., Des. Sel. 19*, 299−307.

(16) Rosenberg, A. (2006) Effects of protein aggregates: An immunologic perspective. *AAPS J. 8*, E501−E507.

(17) Lazar, A. C., Wang, L., Blattler, W. A., Amphlett, G., Lambert, J. M., and Zhang, W. (2005) Analysis of the composition of immunoconjugates using size-exclusion chromatography coupled to mass spectrometry. *Rapid Commun. Mass Spectrom. 19*, 1806−1814.

(18) Wakankar, A. A., and Borchardt, R. T. (2006) Formulation considerations for proteins susceptible to asparagine deamidation and aspartate isomerization. *J. Pharm. Sci. 95*, 2321−2336.

(19) Hunt, G., Moorhouse, K. G., and Chen, A. B. (1996) Capillary isoelectric focusing and sodium dodecyl sulfate-capillary gel electrophoresis of recombinant humanized monoclonal antibody HER2. *J. Chromatogr., A 744*, 295−301.

(20) Harris, R. J., Kabakoff, B., Macchi, F. D., Shen, F. J., Kwong, M., Andya, J. D., Shire, S. J., Bjork, N., Totpal, K., and Chen, A. B. (2001) Identification of multiple sources of charge heterogeneity in a recombinant antibody. *J. Chromatogr., B 752*, 233−245.

(21) Lyubarskaya, Y., Houde, D., Woodard, J., Murphy, D., and Mhatre, R. (2006) Analysis of recombinant monoclonal antibody isoforms by electrospray ionization mass spectrometry as a strategy for streamlining characterization of recombinant monoclonal antibody charge heterogeneity. *Anal. Biochem. 348*, 24−39.

(22) Kumar, S., Ma, B., Tsai, C.-J., and Nussinov, R. (2000) Electrostatic strengths of salt bridges in thermophilic and mesophilic glutamate dehydrogenase monomers. *Proteins: Struct., Funct., Bioinf. 38*, 368−383.

(23) Clark, A. T., Smith, K., Muhandiram, R., Edmondson, S. P., and Shriver, J. W. (2007) Carboxyl pK(a) values, ion pairs, hydrogen bonding, and the pH-dependence of folding the hyperthermophile proteins Sac7d and Sso7d. *J. Mol. Biol. 372*, 992−1008.

(24) Dominy, B. N., Minoux, H., and Brooks, C. L. (2004) An electrostatic basis for the stability of thermophilic proteins. *Proteins: Struct., Funct., Bioinf. 57*, 128−141.

(25) Yadav, S., Laue, T. M., Kalonia, D. S., Singh, S. N., and Shire, S. J. (2012) The influence of charge Distribution on self-association and viscosity behavior of monoclonal antibody solutions. *Mol. Pharmaceutics 9*, 791−802.

(26) Yadav, S., Shire, S. J., and Kalonia, D. S. (2012) Viscosity behavior of high-concentration monoclonal antibody solutions: correlation with interaction parameter and electroviscous effects. *J. Pharm. Sci. 101*, 998−1011.

(27) Maeda, E., Urakami, K., Shimura, K., Kinoshita, M., and Kakehi, K. (2010) Charge heterogeneity of a therapeutic monoclonal antibody conjugated with a cytotoxic antitumor antibiotic, calicheamicin. *J. Chromatogr., A 1217*, 7164−7171.

(28) Stan, A. C., Radu, D. L., Casares, S., Bona, C. A., and Brumeanu, T.-D. (1999) Antineoplastic efficacy of doxorubicin enzymatically assembled on galactose residues of a monoclonal antibody specific for the carcinoembryonic antigen. *Cancer Res. 59*, 115−121.

(29) Liu, J., Zhao, H., Volk, K. J., Klohr, S. E., Kerns, E. H., and Lee, M. S. (1996) Analysis of monoclonal antibody and immunoconjugate digests by capillary electrophoresis and capillary liquid chromatography. *J. Chromatogr., A 735*, 357−366.

(30) Chih, H. W., Gikanga, B., Yang, Y., and Zhang, B. (2011) Identification of amino acid residues responsible for the release of free drug from an antibody-drug conjugate utilizing lysine-succinimidyl ester chemistry. *J. Pharm. Sci. 100*, 2518−2525.

(31) Hamann, P. R., Hinman, L. M., Hollander, I., Beyer, C. F., Lindh, D., Holcomb, R., Hallett, W., Tsou, H.-R., Upeslacis, J., Shochat, D., Mountain, A., Flowers, D. A., and Bernstein, I. (2001) Gemtuzumab ozogamicin, a potent and selective anti-CD33 antibody−calicheamicin conjugate for treatment of acute myeloid leukemia. *Bioconjugate Chem. 13*, 47−58.

(32) Wang, L., Amphlett, G., Blättler, W. A., Lambert, J. M., and Zhang, W. (2005) Structural characterization of the maytansinoid−monoclonal antibody immunoconjugate, huN901−DM1, by mass spectrometry. *Protein Sci. 14*, 2436−2446.

(33) Tanford, C. (1957) Theory of protein titration curves. II. Calculations for simple models at low ionic strength. *J. Am. Chem. Soc. 79*, 5340−5347.

(34) Tanford, C. (1957) The location of electrostatic charges in kirkwood's model of organic ions. *J. Am. Chem. Soc. 79*, 5348−5352.

(35) Tanford, C., and Kirkwood, J. G. (1957) Theory of protein titration curves. I. General equations for impenetrable spheres. *J. Am. Chem. Soc. 79*, 5333−5339.

(36) Saphire, E. O., Parren, P. W. H. I., Pantophlet, R., Zwick, M. B., Morris, G. M., Rudd, P. M., Dwek, R. A., Stanfield, R. L., Burton, D. R., and Wilson, I. A. (2001) Crystal structure of a neutralizing human IgG against HIV-1: A template for vaccine design. *Science 293*, 1155−1159.

(37) Liu, D., Ren, D., Huang, H., Dankberg, J., Rosenfeld, R., Cocco, M. J., Li, L., Brems, D. N., and Remmele, R. L. (2008) Structure and stability changes of human IgG1 Fc as a consequence of methionine oxidation. *Biochemistry 47*, 5088−5100.

(38) Gunasekaran, K., Pentony, M., Shen, M., Garrett, L., Forte, C., Woodward, A., Ng, S. B., Born, T., Retter, M., Manchulenko, K., Sweet, H., Foltz, I. N., Wittekind, M., and Yan, W. (2010) Enhancing antibody Fc heterodimer formation through electrostatic steering effects: applications to bispecific molecules and monovalent IgG. *J. Biol. Chem. 285*, 19637−19646.